

Electronic Structure of Vortices Pinned by Columnar Defects.

A. S. Mel'nikov,¹ A. V. Samokhvalov,¹ and M. N. Zubarev¹

¹*Institute for Physics of Microstructures, Russian Academy of Sciences, 603950 Nizhny Novgorod, GSP-105, Russia*
(Dated: October 28, 2018)

The electronic structure of a vortex line trapped by an insulating columnar defect in a type-II superconductor is analysed within the Bogolubov-de Gennes theory. For quasiparticle trajectories with small impact parameters defined with respect to the vortex axis the normal reflection of electrons and holes at the defect surface results in the formation of an additional subgap spectral branch. The increase in the impact parameter at this branch is accompanied by the decrease of the excitation energy. When the impact parameter exceeds the radius of the defect this branch transforms into the Caroli-de Gennes-Matricon one. As a result, the minigap in the quasiparticle spectrum increases with the increase in the defect radius. The scenario of the spectrum transformation is generalized for the case of arbitrary vorticity.

PACS numbers: 74.45.+c, 74.78.Na, 74.78.-w

I. INTRODUCTION

The study of magnetic and transport properties of type-II superconductors in the presence of artificial pinning centers is known to be an important direction in the physics of vortex matter¹. The artificial pinning provides a unique possibility to control the critical parameters of superconducting materials which are important in various applications. For instance, the critical current j_c and the irreversibility field H_{irr} can be enhanced by the inclusion of normal particles and nanorods^{2,3}, by introducing arrays of submicrometer holes^{4,5}, and by proton⁶ and heavy-ion irradiation⁷. Pinning of flux lines appears to be especially strong for the case of columnar defects elongated nearly parallel to the applied magnetic field, when vortices can be pinned over their entire length. These columnar defects are now widely used to trap vortices and to increase the current carrying capacity of superconductors.

Within the London approximation the interaction between a single vortex and an insulating cylindrical cavity of radius $R \ll \lambda$, where λ is the London penetration depth, was considered in the pioneering paper⁸ for bulk type-II superconductors. For a multiquantum vortex it was shown⁸ that the maximum number of flux quanta which can be trapped by the cylindrical cavity is restricted by the value $R/2\xi$, where ξ is the superconducting coherence length. The generalization of the results of Ref.⁸ for cylindrical cavities of radii $R \gtrsim \lambda$ has been obtained in Ref.⁹. An efficient image method appropriate for the analysis of the vortex-defect interaction in the limit of rather large λ values has been developed in^{10,11}. The formation of superconducting nuclei with nonzero vorticities near the columnar defects or in perforated films has been studied in Refs.^{12,13}.

Certainly the phenomenological approaches used in most of the works cited above can not describe the electronic structure of the vortex states in the presence of small cavities or columnar defects of the radius smaller than the coherence length ξ . This issue is closely related to the problem of microscopic nature of pinning

addressed previously in Ref.¹⁴ for a particular case of point-like defects with the scattering cross section much smaller than the ξ^2 value. An appropriate modification of the quasiparticle spectra caused by a single impurity atom placed in a vortex core has been studied in¹⁵. The case of vortices trapped by normal metal cylindrical defects has been addressed in^{16,17}. The interest to microscopic calculations of electronic structure of the vortex states is stimulated by low-temperature scanning tunneling microscopy (STM) experiments which provide detailed spatially resolved excitation spectra^{18,19,20}. The modern STM techniques could provide us the information about the number and configuration of the spectral branches crossing the Fermi level. Recent STM experiments on NbSe₂ single crystals with a regular array of submicron Au antidots have provided images of both single quantum Abrikosov vortices and multiquanta vortex states forming near normal antidots²¹.

The goal of our paper is to analyse the transformation of the quasiparticle excitation spectra which occurs in a vortex pinned by a columnar defect of finite radius $R \lesssim \xi$. We focus on the modification of the anomalous energy branches caused by normal reflection of quasiparticles at the columnar defect boundary. To elucidate the key points of the present work we start from the qualitative discussion of the spectrum transformation scenario. Let us consider a vortex pinned at an isolating cylinder of a radius R (see Fig.1). The spectrum of quasiparticle states can be analysed considering one-dimensional quantum mechanics of electrons and holes along a set of linear quasiclassical trajectories. Each trajectory is defined by the impact parameter b and the trajectory orientation angle (see Fig.1). For small impact parameters $b < R$ the trajectories experience a normal reflection from the defect surface. Hereafter we assume this reflection to be specular. Far from the reflection point O the superconducting gap is homogeneous ($\Delta = \Delta_0$) and the corresponding superconducting phase difference $\delta\varphi$ between the trajectory ends is defined by the impact parameter b : $\delta\varphi = 2 \arcsin(|b|/R)$. Neglecting the details of the inhomogeneous profile of the order param-

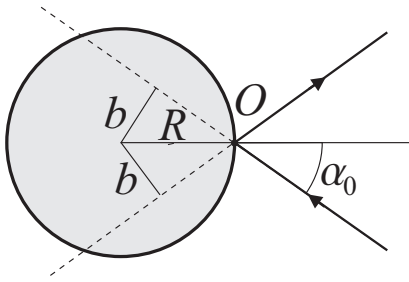


FIG. 1: Specular reflection of a quasiclassical trajectory at the defect surface.

eter inside the vortex core we can take the gap function in the form: $\Delta(s) = \Delta_0 \exp(i \arcsin(|b|/R) \text{sign } s)$, where s is the coordinate changing along the trajectory. The one-dimensional quantum mechanical problem with such order parameter is equivalent to the one describing a single mode Josephson constriction²². The subgap spectrum in this case is known to consist of two energy branches: $\varepsilon_J^\pm(b) = \pm \Delta_0 \cos(\delta\varphi/2) = \pm \Delta_0 \sqrt{1 - b^2/R^2}$, which correspond to the opposite momenta of quasiparticles propagating along the trajectory. Thus, for small impact parameters the scattering of quasiparticles at the defect surface is expected to result in the formation of new energy branches which are splitted from the continuum. Taking the quasiclassical trajectories with large impact parameters $b > R$ one can see that these trajectories are not perturbed by the scattering at the defect and, as a consequence, the spectrum in this case should be described by the well-known Caroli-de Gennes-Matricon (CdGM) expression²³. The crossover between two different regimes occurs in the region $b \sim \pm R$, which should be certainly treated more accurately (see below). One can expect that in this region the CdGM energy branch $\varepsilon_0(b)$ is cut at the energies $\varepsilon \sim \pm \varepsilon_0(R)$ and transforms into the spectral branches ε_J^\pm approaching $\pm \Delta_0$ with the further decrease in the $|b|$ value. The resulting spectrum as a function of a continuous parameter b does not cross the Fermi level: there appears a minigap $\sim \varepsilon_0(R)$. For $R \ll \xi$ this minigap can be approximately written as: $\varepsilon_0(R) \simeq \Delta_0 R/\xi$. The increase in the defect radius is accompanied by the minigap increase and for $R \gg \xi$ all the subgap states appear to be only weakly splitted from the $\pm \Delta_0$ value.

The paper is organized as follows. In Sec. II we briefly discuss the basic equations used for the spectrum calculation. In Sec. III we study the quasiparticle spectrum transformation for a singly quantized vortex pinned at a columnar defect. In Sec. IV we generalize our analysis for the case of a multiquantum vortex trapped by the defect. We summarize our results in Sec. V.

II. BASIC EQUATIONS

Hereafter we consider a columnar defect as an insulating infinite cylinder of the radius R . The magnetic

field \mathbf{B} is assumed to be parallel to the cylinder axis z . We assume the system to be homogeneous along the z -axis, thus, the k_z -projection of the momentum is conserved. The quantum mechanics of quasiparticle excitations in a superconductor is governed by the two dimensional BdG equations for particlelike (u) and holelike (v) parts of the two-component quasiparticle wave functions $\hat{\Psi}(\mathbf{r}, z) = (u, v) \exp(ik_z z)$:

$$-\frac{\hbar^2}{2m} (\nabla^2 + k_\perp^2) u + \Delta(\mathbf{r}) v = \epsilon u \quad (1a)$$

$$\frac{\hbar^2}{2m} (\nabla^2 + k_\perp^2) v + \Delta^*(\mathbf{r}) u = \epsilon v. \quad (1b)$$

Here $\nabla = \partial_x \mathbf{x}_0 + \partial_y \mathbf{y}_0$, $\mathbf{r} = (x, y)$ is a radius vector in the plane perpendicular to the cylinder axis, $\Delta(\mathbf{r})$ is the gap function, and $k_\perp^2 = k_F^2 - k_z^2$.

Following the procedure described in^{24,25,26} we introduce the momentum representation:

$$\hat{\psi}(\mathbf{r}) = \begin{pmatrix} u \\ v \end{pmatrix} = \frac{1}{(2\pi\hbar)^2} \int d^2\mathbf{p} e^{i\mathbf{p}\mathbf{r}/\hbar} \hat{\psi}(\mathbf{p}) \quad (2)$$

where $\mathbf{p} = |\mathbf{p}| (\cos \theta_p, \sin \theta_p) = p \mathbf{p}_0$. The unit vector \mathbf{p}_0 parametrized by the angle θ_p defines the trajectory direction in the (x, y) plane. We assume that our solutions correspond to the momentum absolute values p close to the value $\hbar k_\perp$: $p = \hbar k_\perp + q$ ($|q| \ll \hbar k_\perp$). As a next step, we introduce a Fourier transformation:

$$\hat{\psi}(\mathbf{p}) = \frac{1}{k_\perp} \int_{-\infty}^{+\infty} ds e^{i(k_\perp - |\mathbf{p}|/\hbar)s} \hat{\psi}(s, \theta_p). \quad (3)$$

Finally, the wave function in the real space $\mathbf{r} = r(\cos \theta, \sin \theta)$ is expressed from Eqs.(2, 3) in the following way (see Ref.²⁵):

$$\hat{\psi}(r, \theta) = \int_0^{2\pi} e^{ik_\perp r \cos(\theta_p - \theta)} \hat{\psi}(r \cos(\theta_p - \theta), \theta_p) \frac{d\theta_p}{2\pi}, \quad (4)$$

where (r, θ, z) is a cylindrical coordinate system. The boundary condition at the surface of the insulating cylinder requires

$$\hat{\psi}(R, \theta) = \begin{pmatrix} u \\ v \end{pmatrix}_{r=R} = \frac{1}{2\pi} \int_0^{2\pi} d\theta_p e^{ik_\perp R \cos(\theta_p - \theta)} \hat{\psi}(R \cos(\theta_p - \theta), \theta_p) = 0. \quad (5)$$

To obtain the Andreev equations along the trajectories we look for a solution in the eikonal approximation

$$\hat{\psi}(s, \theta_p) = e^{iS(\theta_p)} \hat{g}(s, \theta_p)$$

assuming \hat{g} to be a slowly varying function of θ_p . Quasiparticles propagating along the classical trajectories parallel to $\mathbf{k}_\perp = k_\perp (\cos \theta_p, \sin \theta_p)$ are characterized by the angular momentum $\mu = -k_\perp b$, where

$$b = -\frac{1}{k_\perp} \frac{\partial S}{\partial \theta_p} \quad (6)$$

is the trajectory impact parameter. Assuming the vortex axis to coincide with the cylinder axis we obtain the axially-symmetric problem with the conserved angular momentum μ .

Finally, the quasiclassical equations for the envelope $\hat{g}(s, \theta_p)$ read:

$$-i\hbar V_{\perp} \hat{\sigma}_z \frac{\partial \hat{g}}{\partial s} + \hat{\sigma}_x \text{Re} \Delta(\mathbf{r}) \hat{g} - \hat{\sigma}_y \text{Im} \Delta(\mathbf{r}) \hat{g} = \left(\epsilon + \frac{\hbar \omega_H}{2} \mu \right) \hat{g}, \quad (7)$$

where $\hat{\sigma}_i$ are the Pauli matrices, $mV_{\perp} = \hbar k_{\perp}$, $\omega_H = |e|H/mc$ is the cyclotron frequency, and

$$x = s \cos \theta_p - b \sin \theta_p, \quad y = s \sin \theta_p + b \cos \theta_p, \\ x \pm iy = (s \pm ib) e^{\pm i\theta_p}.$$

The term proportional to ω_H can be included to the energy as an additive constant (see also²⁷):

$$\epsilon = \epsilon + \frac{\hbar \omega_H}{2} \mu.$$

Our further analysis of quasiparticle excitations is based on the Andreev equations (7) which must be supplemented by the boundary condition (5).

III. SINGLY QUANTIZED VORTEX PINNED BY A COLUMNAR DEFECT

We now proceed with the analysis of the subgap spectrum for a singly quantized vortex trapped by the columnar defect of the radius R . The order parameter $\Delta(x, y)$ takes the form

$$\Delta = \Delta_0 \delta_v(r) e^{i\theta}, \quad r = \sqrt{x^2 + y^2} \geq R. \quad (8)$$

Here $\delta_v(r)$ is a normalized order parameter magnitude for a vortex centered at $r = 0$, such that $\delta_v(r) = 1$ for $r \rightarrow \infty$. In (s, θ_p) variables one obtains for $r = \sqrt{s^2 + b^2} \geq R$:

$$\Delta = D_b(s) e^{i\theta_p}, \quad D_b(s) = \Delta_0 \frac{\delta_v(\sqrt{s^2 + b^2})}{\sqrt{s^2 + b^2}} (s + ib). \quad (9)$$

The cylindrical symmetry of our system allows to separate the θ_p -dependence of the function \hat{g} :

$$\hat{g}(s, \theta_p) = e^{i\hat{\sigma}_z \theta_p / 2} \hat{f}(s). \quad (10)$$

The total wave function $\hat{\psi}(s, \theta_p)$ should be single valued and, thus, the angular momentum μ is half an odd integer. The quasiclassical equations (7) take the form

$$-i\hbar V_{\perp} \hat{\sigma}_z \partial_s \hat{f} + \hat{\Delta}_b(s) \hat{f} = \epsilon \hat{f}, \quad (11)$$

where

$$\hat{\Delta}_b(s) = \hat{\sigma}_x \text{Re} D_b(s) - \hat{\sigma}_y \text{Im} D_b(s) \quad (12)$$

is the gap operator. Changing the sign of the coordinate s one can observe a useful symmetry property of the solution of Eq.(11):

$$\hat{f}(-s) = C \hat{\sigma}_y \hat{f}(s), \quad (13)$$

where C is an arbitrary constant.

A. Boundary condition.

As a next step we rewrite the boundary condition (5) for wave functions $\hat{f}(s)$ defined at the trajectories. Replacing θ_p by $\alpha = \theta_p - \theta$ and shifting the limits of integration in Eq.(5) we find:

$$\int_0^{2\pi} d\alpha e^{ik_{\perp} R \cos \alpha + i\mu \alpha} \left[e^{i\hat{\sigma}_z \alpha / 2} \hat{f}(R \cos \alpha) \right] = 0. \quad (14)$$

Assuming $k_{\perp} R \gg 1$ and the function $e^{i\hat{\sigma}_z \alpha / 2} \hat{f}(s)$ to vary slowly at the atomic length scale we evaluate the above integral using the stationary phase method. For a given value of angular momentum μ the stationary phase points are given by the condition: $\sin \alpha_{1,2} = \mu / k_{\perp} R = -b/R$. One can see that for $|b| > R$ the stationary phase points disappear and, as a result, the integral (14) is always vanishingly small. In this case the boundary condition at the cylinder surface does not impose any restrictions on the wave function \hat{f} defined at the trajectories. In the opposite limit $|b| < R$ one can find two stationary angles $\alpha_1 = \alpha_0 \equiv -\arcsin(b/R)$ and $\alpha_2 = \pi - \alpha_0$ which are in fact the orientation angles for an incident and specularly reflected trajectories shown in Fig. 1. Summing over two contributions we can rewrite the boundary condition (14) as follows:

$$e^{i\hat{\varphi}_1} \hat{f}(s_0) = e^{-i\hat{\varphi}_1} \hat{f}(-s_0), \quad (15)$$

where $s_0 = \sqrt{R^2 - b^2}$, $2\beta_0 = \alpha_0 - \pi/2$ and

$$\hat{\varphi}_1 = k_{\perp} s_0 + (2\mu + \hat{\sigma}_z) \beta_0 - 3\pi/4.$$

B. Solution for large impact parameters $|b| > R$.

In this case the quasiparticle states at the trajectories are not affected by the the normal scattering at the columnar defect boundary and the behavior of an anomalous energy branch is described by the standard CdGM solution for a single Abrikosov vortex. For the sake of completeness we give below the expressions for this spectrum and the corresponding wave functions.

Let us follow the derivation in Ref.²⁸ and consider the imaginary part of the gap operator (12) as a perturbation. Neglecting this term in Eq. (11) we find:

$$-i\hbar V_{\perp} \hat{\sigma}_z \partial_s \hat{f}_0 + \hat{\sigma}_x \text{Re} D_b(s) \hat{f}_0 = \epsilon \hat{f}_0. \quad (16)$$

The above equation has a zero eigenvalue $\varepsilon = 0$ with the following expression for the corresponding normalized eigenfunction \hat{f}_0 :

$$\hat{f}_0 = \sqrt{\frac{1}{2I}} \begin{pmatrix} 1 \\ -i \end{pmatrix} e^{-K_0(s)}, \quad (17)$$

where

$$K_0(s) = \frac{1}{\hbar V_\perp} \int_0^s dt \operatorname{Re} D_b(t), \quad I_0 = \int_{-\infty}^{+\infty} ds e^{-2K_0(s)}. \quad (18)$$

The first order perturbation theory gives us the CdGM excitation spectrum $\varepsilon_0(b)$ for $|b| > R$:

$$\varepsilon_0(b) = \frac{b \Delta_0}{I_0} \int_{-\infty}^{+\infty} ds \frac{\delta_v(\sqrt{s^2 + b^2})}{\sqrt{s^2 + b^2}} e^{-2K_0(s)}. \quad (19)$$

C. Solution for small impact parameters $|b| < R$.

In this case the specular reflection at the cylinder surface changes the trajectory direction and strongly modifies the spectrum. The boundary condition at the surface $r = R$ is determined by the equation (15). Let us introduce the function

$$\hat{F}(s) = \begin{cases} e^{+i\hat{\varphi}_1} \hat{f}(s + s_0), & s > 0 \\ e^{-i\hat{\varphi}_1} \hat{f}(s - s_0), & s < 0 \end{cases}, \quad (20)$$

which is defined at the full s axis and appears to be continuous at $s = 0$: $\hat{F}(-0) = \hat{F}(+0)$. The equation for \hat{F} reads:

$$\begin{aligned} -i\hbar V_\perp \hat{\sigma}_z \partial_s \hat{F} + \hat{\sigma}_x \operatorname{Re} G(s) \hat{F} \\ - \hat{\sigma}_y \operatorname{Im} G(s) \hat{F} = \varepsilon \hat{F}, \end{aligned} \quad (21)$$

where

$$\begin{aligned} G(s) = -\Delta_0 \frac{\delta_v(\sqrt{(|s| + s_0)^2 + b^2})}{\sqrt{(|s| + s_0)^2 + b^2}} \\ \times \left[sb/R + i \left(R + |s| \sqrt{1 - b^2/R^2} \right) \right]. \end{aligned} \quad (22)$$

Taking the limit of large $|s|$ we find:

$$G(s) = -i\Delta_0 e^{i\alpha_0 |s|/s}. \quad (23)$$

One can see that in agreement with the qualitative arguments given in the Introduction the phase difference between the opposite ends of the trajectory equals to $\delta\varphi = -2\alpha_0 = 2 \arcsin(b/R)$. Provided we neglect the inhomogeneity of the order parameter phase inside the core we find the resulting expression for the spectrum: $\varepsilon = \pm \Delta_0 \sqrt{1 - b^2/R^2}$. Certainly, such simplification does not allow us to study the crossover to the CdGM branch

which occurs at $b \sim \pm R$. To develop an analytical description of this crossover we choose to apply the method used above to derive standard CdGM expressions and based on the perturbation theory with respect to the imaginary part of the gap function. One can expect this method to be most adequate for the crossover region of $b \sim R$. As for the limit $b < R$ we shall check the validity of this method using the comparison with our direct numerical analysis of Eq.(21).

Neglecting the maginary part of G we find an exact solution of the equation (21) corresponding to zero energy $\varepsilon = 0$:

$$\hat{F}_0(s) = \sqrt{\frac{1}{2I}} \begin{pmatrix} 1 \\ i\chi \end{pmatrix} e^{-K(s)}, \quad (24)$$

where

$$K(s) = \frac{\chi}{\hbar V_\perp} \int_0^s dt \operatorname{Re} G(t), \quad I = \int_{-\infty}^{+\infty} ds e^{-2K(s)}, \quad (25)$$

and $\chi = \operatorname{sign} b$. The solutions (24), (25) appear to decay both at negative and positive s and, thus, we get a localized wave function describing a bound state. Using this localized solution as a zero-order approximation for the wave function the spectrum can be found within the first order perturbation theory. Note, that our perturbation procedure fails for $|b| \rightarrow 0$ because of the increase in the localization radius of the wave function (24).

The first-order approximate solution of the quasiclassical equations (21) takes the form:

$$\hat{F}(s) = A \begin{pmatrix} 1 \\ i\chi \end{pmatrix} e^{-K(s)} + B(s) \begin{pmatrix} 1 \\ -i\chi \end{pmatrix} e^{K(s)}, \quad (26)$$

where

$$B(s) = \frac{iA}{\hbar V_\perp} \int_{-\infty}^s dt [\varepsilon - \chi \operatorname{Im} G(t)] e^{-2K(t)}. \quad (27)$$

To avoid the wave function divergence we should put

$$\int_{-\infty}^{\infty} dt [\varepsilon - \chi \operatorname{Im} G(t)] e^{-2K(t)} = 0.$$

This condition gives us the excitation spectrum ε_s as a function of the impact parameter b for $|b| < R$:

$$\begin{aligned} \varepsilon_s(b) = \frac{\chi \Delta_0}{I} \int_{-\infty}^{+\infty} ds \frac{\delta_v(\sqrt{(|s| + s_0)^2 + b^2})}{\sqrt{(|s| + s_0)^2 + b^2}} \\ \times \left(R + |s| \sqrt{1 - b^2/R^2} \right) e^{-2K(s)}. \end{aligned} \quad (28)$$

It is evident that $\varepsilon_s(R) = \varepsilon_0(R)$ and, thus, the expressions (19) and (28) describe the spectrum $\varepsilon(b)$ for an arbitrary impact parameter b :

$$\varepsilon(b) = \begin{cases} \varepsilon_s(b), & |b| \leq R \\ \varepsilon_0(b), & |b| > R \end{cases}. \quad (29)$$

The discontinuity of the derivative $d\varepsilon/db$ at $|b| = R$ appears because of the breakdown of the above quasiclassical description for the rectilinear trajectories touching the surface of the defect.

In figures 2 and 3 we compare the typical plots of quasiparticle spectra obtained analytically, i.e., using Eq.(29), and numerically. The qualitative behavior of the spectrum is weakly sensitive to the concrete gap profile inside the core and, thus, we choose a simple model profile:

$$\delta_v(r) = r/\sqrt{r^2 + \xi_v^2}, \quad (30)$$

where the core size ξ_v equals to the coherence length $\xi = \hbar V_F/\Delta_0$. We plot here only the spectrum for positive energies and k_z momenta because the eigenvalues for $\varepsilon < 0$ and $k_z < 0$ can be found using the spectrum symmetry properties: $\varepsilon(-b, k_z) = -\varepsilon(b, k_z)$ and $\varepsilon(b, -k_z) = \varepsilon(b, k_z)$. To find the spectral branch $\varepsilon(b, k_z)$ numerically we solve quasiclassical equations (11) for $s \geq s_0$ requiring the decay of the wave function \hat{f} at $s \rightarrow \infty$. An appropriate boundary condition for electron f_u and hole f_v components of the wave function $\hat{f} = (f_u, f_v)$ at $s = 0$ can be found from Eq.(15) and the symmetry property (13):

$$f_v(s_0) = e^{i\alpha_0} f_u(s_0). \quad (31)$$

For $|b| > R$ we put $s_0 = 0$, and the boundary condition (31) takes the form $f_v(0) = -i\chi f_u(0)$.

Comparing the spectrum (29) with the branches obtained from the direct numerical analysis of the eigenvalue problem (11), (31) one can see that the perturbation method provides a reasonable description of the

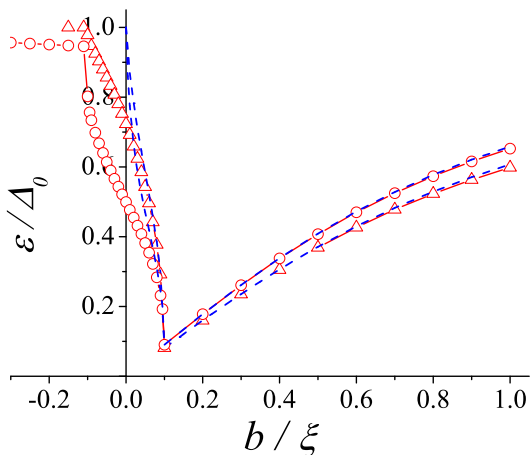


FIG. 2: (Color online) The spectral branches as functions of the impact parameter b , obtained from numerical solution of the eigenvalue problem (11),(31), are shown by red triangles and circles for $k_z = 0$ and $k_z = 0.9k_F$, respectively. The spectral branches calculated using Eq. (29) are shown by blue dash lines. Here we put $R = 0.1\xi$.

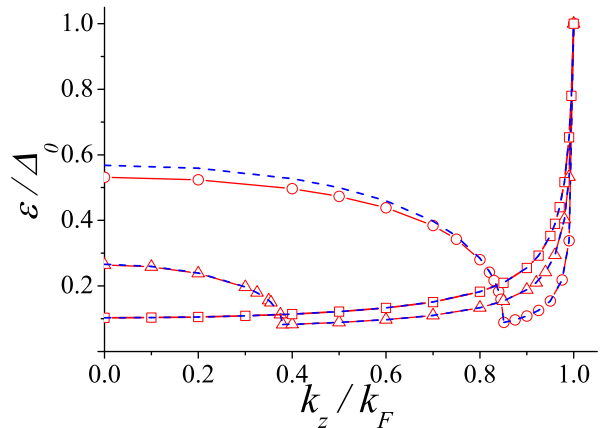


FIG. 3: (Color online) The quasiparticle spectra obtained from the numerical solution of the eigenvalue problem (11), (31) are shown by red circles ($\mu = -10.5$), triangles ($\mu = -18.5$), and squares ($\mu = -25.5$). The spectral branches calculated using Eq. (29) are shown by blue dash lines. Here we put $R = 0.1\xi$, $k_F\xi = 200$.

energy spectrum behavior in a wide range of the impact parameters. As one would expect, the perturbation procedure fails for small impact parameters $|b| \ll R$. Contrary to the CdGM case the spectrum branch (29) does not cross the Fermi level, and the minigap in the quasiparticle spectrum $\Delta_{min} = \varepsilon(R)$ grows with the increase in the cylinder radius R (see Fig. 2). Existence of the minigap in the spectrum of quasiparticles should result in peculiarities of the density of states (DOS) and can be probed by the STM measurements. For $|\mu| < k_FR$ the spectrum $\varepsilon(k_z)$ has a minimum (see Fig. 3), therefore we can expect the appearance of a van Hove singularity in the energy dependence of the DOS.

IV. QUASIPARTICLE SPECTRUM OF A MULTIQUANTUM VORTEX

In this section we generalize the above analysis for the case of a multiquantum vortex pinned by the columnar defect of the radius R . The multiquantum vortices can be trapped at columnar defects either for a rather large defect radius or for the mixed state in mesoscopic samples^{21,29,30,31}. In the absence of defects the spectrum of a multiquantum vortex with the vorticity M is known to consist of M anomalous energy branches²⁸. The behavior of these branches has been previously investigated both numerically and analytically^{16,17,26,32,33}. Here we restrict ourselves by the numerical solution of the eigenvalue problem (11) assuming that the order parameter $\Delta_M(r)$ takes the form

$$\Delta_M(r) = \Delta_0 [\delta_v(r)]^M e^{iM\theta}, \quad r \geq R, \quad (32)$$

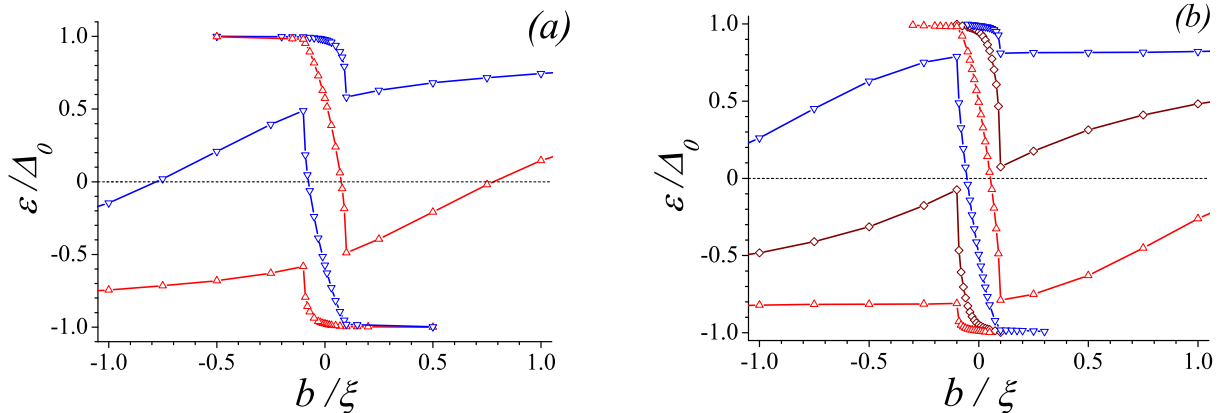


FIG. 4: (Color online) The spectral branches as functions of the impact parameter b , obtained from the numerical solution of the eigenvalue problem (11), (36) for $M = 2$ (a) and $M = 3$ (b) ($R = 0.1\xi$).

where the function $\delta_v(r)$ is determined by the expression (30). In (s, θ_p) variables one obtains for $s \geq s_0$:

$$\Delta_M = D_M(s) e^{iM\theta_p}, \quad (33)$$

$$D_M(s) = \Delta_0 \left[\frac{\delta_v(\sqrt{s^2 + b^2})}{\sqrt{s^2 + b^2}} \right]^M (s + ib)^M. \quad (34)$$

Using the transformation

$$\hat{g}(s, \theta_p) = e^{iM\hat{\sigma}_z\theta_p/2} \hat{f}(s) \quad (35)$$

we can rewrite the quasiclassical equations (7) in the form (11) with the gap operator

$$\hat{\Delta}_b(s) = \hat{\sigma}_x \text{Re}D_M(s) - \hat{\sigma}_y \text{Im}D_M(s). \quad (36)$$

The symmetry properties of both the gap operator $\hat{\Delta}_b(s)$ and the equation (11) depend on the vorticity M :

$$\hat{\Delta}_b(-s) = \begin{cases} \hat{\Delta}_b^*(s), & \text{for even } M \\ -\hat{\Delta}_b^*(s), & \text{for odd } M \end{cases}. \quad (37)$$

This fact allows to obtain the following condition:

$$\hat{f}(-s) = \begin{cases} C \hat{\sigma}_x \hat{f}(s), & \text{for even } M \\ C \hat{\sigma}_y \hat{f}(s), & \text{for odd } M \end{cases}, \quad (38)$$

which generalizes the condition (13) for a multiquantum vortex. Here C is an arbitrary constant. Using the stationary phase method we can write the boundary condition for wave functions $\hat{f}(s)$ at the surface of the insulating cylinder in the form:

$$e^{i\hat{\varphi}_M} \hat{f}(s_0) = e^{-i\hat{\varphi}_M} \hat{f}(-s_0), \quad (39)$$

where

$$\hat{\varphi}_M = k_\perp s_0 + (2\mu + M\hat{\sigma}_z)\beta_0 - 3\pi/4.$$

Taking into account the Eq.(38) the boundary condition (39) can be written for electron f_u and hole f_v components of the wave function \hat{f} :

$$f_v(s_0) = \pm e^{iM\alpha_0} f_u(s_0). \quad (40)$$

For $|b| > R$ we can put here $s_0 = 0$ and $\alpha_0 = -\pi/2$. The choice of the sign in (40) depends on the number of the spectral branch. The typical plots of quasiparticle spectra obtained from numerical solution of the eigenvalue problem (11), (36) with the boundary condition (40) for vortices with winding numbers $M = 2, 3$ are shown in Fig. 4. Similarly to the case of a singly quantized vortex the small b part of the spectrum is formed by the spectral branches induced by the normal scattering at the defect. These branches transform into the standard anomalous ones with the increase in the $|b|$ value. With the increase in the cylinder radius all the spectral branches appear to be expelled from the Fermi level.

V. SUMMARY

To sum up, we described a transformation of the sub-gap spectral branches of quasiparticle excitations in vortices pinned by columnar defects of finite radii. We find that the normal scattering at the defect surface results in the appearance of additional spectral branches which transform into the CdGM one with an increase in the impact parameter of quasiparticle trajectories. The increase in the defect radius is accompanied by the increase in the minigap in the spectrum which can be observed, e.g., in the STM measurements. One can expect that such changes in the spectrum behavior should affect strongly the dynamic mobility of vortices in the presence of ac transport current (see, e.g.,³⁴ for review).

ACKNOWLEDGEMENTS

We are thankful to N. B. Kopnin, A. I. Buzdin, V. M. Vinokur, and G. Karapetrov for stimulating discussions.

This work was supported, in part, by the Russian Foundation for Basic Research and by the “Dynasty” Foundation (A.S.M.).

-
- ¹ G. Blatter, M. V. Feigel'man, V. B. Geshkenbein, A. I. Larkin, V. M. Vinokur, *Rev. Mod. Phys.* **66**, 1125 (1994).
² P. Yang and Ch. M. Lieber, *Science* **273**, 1836-1840 (1996).
³ M. Peurla, H. Huhtinen, M. A. Shakhov, K. Traito, Yu. P. Stepanov, M. Safonchik, P. Paturi, Y. Y. Tse, R. Palai, and R. Laiho, *Phys. Rev. B* **75**, 184524-1-184524-6 (2007).
⁴ A. F. Hebard, A. T. Fiory, and S. Somekh, *IEEE Trans. Magn.* **1**, 589 (1977).
⁵ M. Baert, V. V. Metlushko, R. Jonckheere, V. V. Moshchalkov, and Y. Bruynseraede, *Phys. Rev. Lett.* **74**, 3269-3272 (1995).
⁶ L. Civale, A. D. Marwick, M. W. McElfresh, T. K. Worthington, A. P. Malozemoff, F. Holtzberg, J. R. Thompson, and M. A. Kirk, *Phys. Rev. Lett.* **65**, 1164-1167 (1990).
⁷ L. Civale, A. D. Marwick, T. K. Worthington, M. A. Kirk, J. R. Thompson, L. Krusin-Elbaum, Y. Sun, J. R. Clem, and F. Holtzberg, *Phys. Rev. Lett.* **67**, 648-651 (1990).
⁸ G. S. Mkrtchyan and V. V. Schmidt, *Zh. Eksp. Teor. Fiz.* **61**, 367 (1971) [*Sov. Phys. JETP* **34**, 195 (1972)].
⁹ H. Nordborg and V. M. Vinokur, *Phys. Rev. B* **62**, 12408 (2000).
¹⁰ A. Buzdin and D. Feinberg, *Physica C* **256**, 303 (1996).
¹¹ A. Buzdin and M. Daumens, *Physica C* **294**, 257 (1998).
¹² A. I. Buzdin, *Phys. Rev. B* **47**, 11416 (1993).
¹³ A. Bezryadin, A. Buzdin, and B. Pannetier, *Phys. Lett. A* **195**, 373 (1994).
¹⁴ E. V. Thuneberg, J. Kurkijarvi, and D. Rainer, *Phys. Rev. Lett.* **48**, 1853 (1982); E.V.Thuneberg, J.Kurkijarvi, and D.Rainer, *Phys. Rev. B* **29**, 3913 (1984); E. V. Thuneberg, J. Low Temp. Phys. **57**, 415 (1984); M. Friesen and P. Muzikar, *Phys. Rev. B* **53**, R11953 (1996).
¹⁵ A. I. Larkin and Yu. N. Ovchinnikov, *Phys. Rev. B* **57**, 5457 (1998).
¹⁶ Y. Tanaka, S. Kashiwaya, and H. Takayanagi, *Jpn. J. Appl. Phys. Part 1* **34**, 4566 (1995).
¹⁷ M. Eschrig, D. Rainer, and J. A. Sauls: in *Vortices in unconventional superconductors and superfluids*, ed. R.P. Huebener, N. Schopohl and G.E. Volovik (Springer Verlag, Berlin, 2001), preprint cond-mat/0106546.
¹⁸ H. Hess, R. B. Robinson, R. C. Dynes, J. M. Valles, Jr., and J. Waszczak, *Phys. Rev. Lett.* **62**, 214 (1989).
¹⁹ B. W. Hoogenboom, M. Kugler, B. Revaz, I. Maggio-Aprile, O. Fischer, and Ch. Renner, *Phys. Rev. B* **62**, 9179 (2000).
²⁰ I. Guillamon, H. Suderow, S. Vieira, L. Cario, P. Diener, and P. Rodiere, *Phys. Rev. Lett.* **101**, 166407 (2008).
²¹ G. Karapetrov, J. Fedor, M. Iavarone, D. Rosenmann, and W. K. Kwok, *Phys. Rev. Lett.* **95**, 167002 (2005).
²² C. W. J. Beenakker and H. van Houten, *Phys. Rev. Lett.* **66**, 3056, (1991); C. W. J. Beenakker, *Phys. Rev. Lett.* **67**, 3836, (1991).
²³ C. Caroli, P. G. de Gennes, J. Matricon, *Phys. Lett.* **9**, 307 (1964).
²⁴ A. S. Melnikov, M. A. Silaev, *Pisma Zh. Eksp. Teor. Fiz.* **83**, 675 (2006) [*JETP Lett.* **83**, 578 (2006)].
²⁵ N. B. Kopnin, A. S. Melnikov, V. I. Pozdnyakova, D. A. Ryzhov, I. A. Shereshevskii, and V. M. Vinokur, *Phys. Rev. B* **75**, 024514 (2007).
²⁶ A. S. Mel'nikov, D. A. Ryzhov, and M. A. Silaev, *Phys. Rev. B* **78**, 064513 (2008).
²⁷ Brun E. Hansen, *Phys. Lett. A* **27**, 576 (1968).
²⁸ G. E. Volovik, *Pisma Zh. Eksp. Teor. Fiz.* **57**, 233 (1993) [*JETP Lett.* **57**, 244 (1993)].
²⁹ A. Bezryadin, Yu. N. Ovchinnikov, B. Pannetier, *Phys. Rev. B* **53**, 8553 (1996).
³⁰ A. V. Silhanek, S. Raedts, M. J. Van Bael, and V. V. Moshchalkov, *Phys. Rev. B* **70**, 054515 (2004).
³¹ I. V. Grigorieva, W. Escoffier, V. R. Misko, B. J. Baelus, F. M. Peeters, L. Y. Vinnikov, and S. V. Dubonos, *Phys. Rev. Lett.* **99**, 147003 (2007).
³² Y. Tanaka, A. Hasegawa, and H. Takayanagi, *Solid State Commun.* **85**, 321 (1993); D. Rainer, J. A. Sauls, and D. Waxman, *Phys. Rev. B* **54**, 10094 (1996); S. M. M. Virtanen and M. M. Salomaa, *ibid.* **60**, 14581 (1999); K. Tanaka, I. Robel, and B. Janko, *Proc. Natl. Acad. Sci. U.S.A.* **99**, 5233 (2002).
³³ A. S. Melnikov and V. M. Vinokur, *Nature (London)* **415**, 60 (2002); *Phys. Rev. B* **65**, 224514 (2002).
³⁴ N. B. Kopnin, *Theory of Nonequilibrium Superconductivity* (Clarendon Press, Oxford, 2001).